

PATTERN FORMATION IN ROSENZWEIG–MACARTHUR MODEL WITH PREY–TAXIS

YUANYUAN ZHANG AND LI XIA

Abstract. In this paper we study the existence and stability of nonconstant positive steady states to a reaction–advection–diffusion system with Rosenzweig–MacArthur kinetics. This system can be used to model the spatial–temporal distributions of predator and prey species. We investigate the effect of prey–taxis on the formation of nonconstant positive steady states in 1D. Stability and instability of these nonconstant steady states are also obtained. We also perform some numerical studies to support the theoretical findings. It is also shown that the Rosenzweig–MacArthur prey–taxis model admits very rich and complicated spatial–temporal dynamics.

Key words. Predator–prey, prey–taxis, steady state, stability analysis.

1. Introduction and preliminary results

Recently there has been great interest in the mathematical modeling and analysis of spatial–temporal population distributions of interacting species in biology and ecology. In the world of living things, one of the characteristic features of organisms is their ability to sense the stimulating signals in the environment and adjust movements accordingly. In predator–prey interactions, prey–taxis is the directed movement of predator species along the gradient of high prey population density. Prey–taxis is called positive or prey–attractive if predators move towards and forage the high density prey, while it is called negative or prey–repulsive if predators move against and retreat from preys’ habitat. This is very similar as chemotaxis in which cellular bacteria move in response to chemical stimulus in their environment [11, 13, 15, 21].

We consider a reaction–advection–diffusion system of $u = u(x, t)$ and $v = v(x, t)$ in the following form

$$(1) \quad \begin{cases} u_t = d_1 \Delta u + u(a(1 - \frac{u}{h}) - \frac{bv}{u+c}), & x \in \Omega, t > 0, \\ v_t = \nabla \cdot (d_2 \nabla v - \chi \phi(u, v) \nabla u) + v(\frac{eu}{u+c} - d), & x \in \Omega, t > 0, \\ \partial_{\mathbf{n}} u = \partial_{\mathbf{n}} v = 0 & x \in \partial\Omega, t > 0, \\ u(x, 0) = u_0(x), v(x, 0) = v_0(x), & x \in \Omega, \end{cases}$$

where $\Omega \subset \mathbb{R}^N$, $N \geq 1$, is a bounded domain with smooth boundary $\partial\Omega$; $\Delta = \sum_{i=1}^N \frac{\partial^2}{\partial x_i^2}$ and $\nabla = (\frac{\partial}{\partial x_1}, \dots, \frac{\partial}{\partial x_i}, \dots, \frac{\partial}{\partial x_N})$. d_1, d_2, a, b, c, d, e and h are all positive constants. ϕ is assumed to be a smooth function of u and v , and $\phi(0, v) = 0$ for all $v > 0$, which describes the biologically realistic situation that there is no prey–taxis in the absence of prey species; $\partial_{\mathbf{n}}$ denotes the unit outer normal derivative on the boundary. System (1) is a prey–taxis model, where u and v denote population densities of prey and predator species at space–time location (x, t) respectively. The movement of prey u is purely diffusive, while that of predator v is both diffusive and advective. d_1 and d_2 are random dispersal rates of prey and predator. χ measures the strength of prey–taxis. For example, if $\phi(u, v) > 0$ for all $u, v > 0$,

Received by the editors December 7, 2017 and, in revised form, April 1, 2018.

2000 *Mathematics Subject Classification.* 92C17, 35B32, 35B35, 35B36, 35J47, 35K20, 37K45, 37K50.

then the prey–taxis is positive if $\chi > 0$ and it is negative if $\chi < 0$. Here the potential function ϕ reflects the intensity of such directed dispersal with respect to the variation of both predator and prey densities. We would like to remark the opposite case $\phi(u, v) < 0$ can be used to model volume–filling effect in predators or group–defense in preys. See our discussions in the last paragraph of this section. It is the goal of this paper to study the existence and stability of nonconstant positive solutions to the stationary system of (1).

The reaction system in (1) or its ODE system is referred to as the Rosenzweig–MacArthur model [34, 43]

$$\begin{cases} u_t = u(a(1 - \frac{u}{h}) - \frac{bv}{u+c}), & t > 0, \\ v_t = v(\frac{eu}{u+c} - d), & t > 0, \\ u(0) = u_0, v(0) = v_0, \end{cases}$$

which has been widely applied in real–life ecology [36]. This model is also known as the Lotka–Volterra equations with a Holling type II predator functional response or the Gause model. See [34, 35] and Chap. 4 in [9] for works on this system and similar modified Lotka–Volterra equations. Here a is the intrinsic growth rate of the predator, h is the environment carrying capacity, b and e are the interaction rates for the two species, and d is the intrinsic death rate of the predator. c measures the saturation effect on the predator growth due to the consumption of prey at a unit number.

The Rosenzweig–MacArthur ODE model has been investigated by various authors. It is easy to see that it has three equilibrium points $(0, 0)$, $(h, 0)$ and

$$(2) \quad (\bar{u}, \bar{v}) = \left(\frac{cd}{e-d}, \frac{ace(h(e-d) - cd)}{bh(e-d)^2} \right),$$

where (\bar{u}, \bar{v}) is positive if and only if $0 < cd < h(e-d)$. For the sake of our mathematical analysis, throughout this paper we make the following assumptions

$$(3) \quad d < e, \frac{cd}{e-d} < h < \frac{c(d+e)}{e-d}.$$

By the standard ODE stability analysis, see [9, 17] e.g., the first two equilibrium points $(0, 0)$ and $(h, 0)$, corresponding to the extinction of species and predators respectively, are both saddle points. (\bar{u}, \bar{v}) corresponds to the coexistence of both species and it undergoes a Hopf bifurcation as e increases. Moreover, according to [2], this equilibrium loses its stability to a small amplitude periodic orbit which is unique hence stable. The relaxation oscillator profile of the unique limit cycle of the ODE system is discussed in [16]. See [57] and the references therein for more discussions. We also want to point out that Rinaldi *et al.* [42] studied this model with time–periodically varying parameters and identified six elementary seasonality mechanisms through complete bifurcation diagrams.

In the absence of prey–taxis, system (1) reads

$$(4) \quad \begin{cases} u_t = d_1 \Delta u + u(a(1 - \frac{u}{h}) - \frac{bv}{u+c}), & x \in \Omega, t > 0, \\ v_t = d_2 \Delta v + v(\frac{eu}{u+c} - d), & x \in \Omega, t > 0, \\ \partial_{\mathbf{n}} u = \partial_{\mathbf{n}} v = 0 & x \in \partial\Omega, t > 0, \\ u(x, 0) = u_0(x), v(x, 0) = v_0(x), & x \in \Omega, \end{cases}$$

and this model has also been extensively studied by various authors. Choosing $d_2 = 0$ and scaling the rest parameters in (4), Dunbar [7] obtained periodic traveling wave train and traveling front solutions for this diffusive predator–prey system. His analysis also shows the existence of periodic orbits, heteroclinic orbits and a

heteroclinic connection of a point and a periodic orbit. Yi *et al.* [57] performed detailed bifurcation analysis to general reaction–diffusion one–dimensional systems including the diffusive system (4). They derived an explicit algorithm to determine the properties of Hopf bifurcation of general reaction–diffusion systems (without cross–diffusion) through very detailed and complete calculations which are convenient for readers and future applications. Steady state bifurcations are carried out in details. See [57] and the references therein for more works of reaction–diffusion systems arising from population dynamics.

From the view point of mathematical modeling, it is interesting and important to study formation of nontrivial patterns in the reaction–diffusion systems of population dynamics. These patterns can be used to describe various interesting phenomena such as specific segregation which is ubiquitous in ecosystems. Coexistence of prey and predator species, which is crucial to biodiversity of an ecosystem, can be modeled by spatially inhomogeneous positive patterns. We are motivated to study the existence and stability of nonconstant positive steady states of (1) which are natural candidates for the attractors of the time–dependent system. In particular we investigate the effect of prey–taxis on the pattern formations in (4). Though it is accepted by many scholars that mathematical analysis of prey–taxis system including (1) was initiated by Ainseba *et al.* [1] in 2008, reaction–diffusion systems with prey–taxis have been proposed and studied by various authors much earlier as far as we know. For example, Kareiva and Odell [19] in 1987 proposed a mechanistic approach formulated as PDEs with spatially varying dispersals and advection to demonstrate and explain that area–restricted search does create predator aggregation. Moreover, chemotaxis modeling the directed movement of cells to stimulating chemicals has been mathematically modeled by Patlak [40] in the 1950s and Keller–Segel [21, 22, 23] early in the 1970s.

There are some works devoted to the mathematical analysis of prey–taxis models. In [1], Ainseba *et al.* proved the existence of weak solutions of system (1) with slightly general kinetics through Schauder fixed point theorem and the uniqueness of the weak solution via duality technique. It is assumed that the sensitivity function takes the form $\phi(u, v) = u\phi_1(v)$ and there exists a threshold value v_m (denoted by u_m in [1]) such that $\phi_1(v) \equiv 0$ for all $v \geq v_m$. This assumption contributes to the mathematical analysis in [1] and it is reasonable with biology justifications. It is sometimes referred to (e.g., [38]) as the volume–filling effect in predation which models the situation that predators stop foraging self–packed environment and prey–taxis vanishes there. Under the same volume–filling assumption, Tao [48] obtained global existence and uniqueness to this system through contraction mapping principle. Recently, He and Zheng [14] further proved that the global solution obtained in [48] is globally bounded when the space dimension $N = 1, 2, 3$. Lee *et al.* studied pattern formation in [29] and traveling wave solutions in [30] for 1D prey–taxis systems with several classes of population kinetics. It is showed that prey–taxis stabilizes population dynamics and inhibits formation of nontrivial patterns when there is no prey–repulsion such as aforementioned volume–filling effect. Yousefnezhad and Mohammadi [58] studied global asymptotic stability of the positive equilibrium for systems with general kinetics than (1). By the Crandall–Rabinowitz theory [5, 6] and the user–friendly version developed by Shi and Wang [46], bifurcation analysis is carried out in [55] for (1) with $\phi(u, v) \equiv \chi(u)$, χ being an arbitrary constant (not necessary positive) over multi–dimensions. Li *et al.* [31] investigated global stabilities of equilibrium points to (1) with volume–filling effect. They also carried out detailed Hopf bifurcation analysis following the algorithm

developed in [57]. Existence of non-constant positive steady states is obtained through degree method there. It seems necessary to mention that [52] considered a very similar prey-taxis model with slightly different kinetics. Both our theoretical and numerical results indicate that prey-taxis induces various complicated and complex spatial-temporal dynamics, which might share similarities even when the kinetics are different. For predator-prey models with (non)linear diffusion, other types of population kinetics, or population dynamics model with heterogeneous environment, see the works [4, 10, 25, 26, 27, 28, 37, 44] and the references therein.

It is the goal of our paper to investigate the existence and stability of non-constant positive steady states to (1). For the simplicity of mathematics and better illustration of our theoretical and numerical results, we shall confine our attention to system (1) over one-dimensional interval $(0, L)$

$$(5) \quad \begin{cases} u_t = d_1 u_{xx} + u(a(1 - \frac{u}{h}) - \frac{bv}{u+c}), & x \in (0, L), t > 0, \\ v_t = (d_2 v_x - \chi \phi(u, v) u_x)_x + v(\frac{eu}{u+c} - d), & x \in (0, L), t > 0, \\ u_x = v_x = 0 & x = 0, L, t > 0, \\ u(x, 0) = u_0(x), v(x, 0) = v_0(x), & x \in (0, L). \end{cases}$$

The starting point in our analysis of (5) is the linearized stability of the equilibrium (\bar{u}, \bar{v}) . In the mathematical analysis of pattern formation in reaction-diffusion systems, principle of exchange of stability is often employed to determine when bifurcation occurs for a class of evolutionary equations. See [45, 47] etc. for example. It is well known that Turing's instability can be applied for the pattern formation in various reaction-diffusion systems, however, when Turing's instability does not occur in the purely diffusive system, advection tends to destabilize the spatially homogeneous solutions as certain system bifurcation parameter crosses a threshold value, then there emerge spatially inhomogeneous solutions to the system. Moreover this principle usually gives a qualitative relationship between the shape of bifurcating curve (such as its turning direction) of solutions and their stability.

There are several contributions of the current work. First of all, our linearized stability analysis of equilibrium (\bar{u}, \bar{v}) extends the results in [30] which states that prey-taxis stabilizes reaction-advection-system including (1). Our analysis shows that this is true only if the prey-taxis is positive, however this conclusion does not hold when prey-repulsion is taken into consideration, which models the biologically realistic volume-filling effect due to the over-crowding of predator species or group defense of prey species. Then we apply bifurcation theory to obtain nonconstant positive steady states to (1). See Theorem 2.2. Our stability analysis of the bifurcating solutions in Theorem 3.1 provides a wave mode selection mechanism for (1), following the approach recently developed in [32, 51, 54] etc. for reaction-advection-diffusion systems modeling chemotaxis or species competition. Since our work is in 1D, Neumann Laplacian eigenvalue is $-(\frac{k\pi}{L})^2$ and it has a very clean structure, therefore we are able to perform detailed and involved calculations to show that the bifurcation branches are pitch-fork, in contrast to the transcritical branches in [55]. We shall show that the only stable local branch must have a critical bifurcation value and its stability is determined by its turning direction. Finally, we perform extensive numerical simulations in Section 4 to illustrate and support our theoretical results. Our numerical studies of (5) indicate that this 1D prey-taxis system admits very complicating and interesting spatial-temporal dynamics.

2. Existence of nonconstant positive steady state

This section is devoted to obtain existence of nonconstant positive steady states of (5), i.e., nonconstant positive solutions to the following system

$$(6) \quad \begin{cases} d_1 u'' + u(a(1 - \frac{u}{h}) - \frac{bv}{u+c}) = 0, & x \in (0, L), \\ (d_2 v' - \chi \phi(u, v) u')' + v(\frac{cu}{u+c} - d) = 0, & x \in (0, L), \\ u' = v' = 0, & x = 0, L, \end{cases}$$

where $'$ denotes $\frac{d}{dx}$ here and in the sequel. In particular, we are interested in the effect of prey-taxis on the qualitative behaviors of the solutions.

2.1. Linearized stability analysis of homogeneous steady state. We first investigate linearized analysis of its homogeneous solution (\bar{u}, \bar{v}) given by (2). Take $(u, v) = (\bar{u}, \bar{v}) + (U, V)$, where U and V are small spatial perturbations in $H^2(0, L) \times H^2(0, L)$, then we arrive at the following system

$$(7) \quad \begin{cases} U_t \approx d_1 U_{xx} + (a(1 - \frac{2\bar{u}}{h}) - \frac{bc\bar{v}}{(\bar{u}+c)^2})U - \frac{b\bar{u}}{\bar{u}+c}V + O(U^2), & x \in (0, L), t > 0 \\ V_t \approx (d_2 V_x - \chi \phi(\bar{u}, \bar{v}) U_x)_x + \frac{ce\bar{v}}{(\bar{u}+c)^2}U + \frac{\bar{u}(e-d)-cd}{\bar{u}+c}V + O(V^2), & x \in (0, L), t > 0 \\ U_x(x) = V_x(x) = 0, & x = 0, L, t > 0. \end{cases}$$

Now we look for solutions of (7) in the form

$$(U, V) = (C_1, C_2)e^{\sigma t + i\mathbf{k}x},$$

where C_i ($i = 1, 2$) are constants to be determined, σ is the growth rate of the perturbations and \mathbf{k} is the wavemode vector with $|\mathbf{k}|^2 = (\frac{k\pi}{L})^2$. Substituting these solutions into the linearized system (7) and equate their first order terms, we have

$$(\sigma I + \mathcal{A}_k) \begin{pmatrix} C_1 \\ C_2 \end{pmatrix} = \begin{pmatrix} 0 \\ 0 \end{pmatrix},$$

where the stability matrix is

$$(8) \quad \mathcal{A}_k = \begin{pmatrix} -d_1(\frac{k\pi}{L})^2 - \frac{a}{h}\bar{u} + \frac{b\bar{u}\bar{v}}{(\bar{u}+c)^2} & -\frac{b\bar{u}}{\bar{u}+c} \\ \chi \phi(\bar{u}, \bar{v})(\frac{k\pi}{L})^2 + \frac{ce\bar{v}}{(\bar{u}+c)^2} & -d_2(\frac{k\pi}{L})^2 \end{pmatrix}, k \in \mathbb{N}.$$

By the standard principle of linearized stability (Theorem 5.2 in [47] or [45] e.g.), (\bar{u}, \bar{v}) is asymptotically stable with respect to (1) if and only if the real part of the eigenvalue σ to matrix (8) is negative for any $k \in \mathbb{N}^+$. The characteristic polynomial to (8) reads

$$(9) \quad p_k(\sigma) = \sigma^2 - T_k \sigma + D_k,$$

where

$$T_k = -(d_1 + d_2)(\frac{k\pi}{L})^2 - \frac{a}{h}\bar{u} + \frac{b\bar{u}\bar{v}}{(\bar{u}+c)^2}$$

and

$$D_k = \left(d_1(\frac{k\pi}{L})^2 + \frac{a}{h}\bar{u} - \frac{b\bar{u}\bar{v}}{(\bar{u}+c)^2} \right) d_2(\frac{k\pi}{L})^2 + \left(\chi \phi(\bar{u}, \bar{v})(\frac{k\pi}{L})^2 + \frac{ce\bar{v}}{(\bar{u}+c)^2} \right) \frac{b\bar{u}}{\bar{u}+c}.$$

We notice that $T_k < 0$ for each $k \in \mathbb{N}$ thanks to (3). According to the standard linearized stability theory, since $D_0 > 0$, (\bar{u}, \bar{v}) is locally stable if and only if $D_k > 0$ for each $k \in \mathbb{N}^+$, while it is unstable if there exists at least one k such that $D_k < 0$. We have the following results.

Lemma 2.1. *Suppose that condition (3) holds and $\phi(\bar{u}, \bar{v}) \neq 0$. If $\phi(\bar{u}, \bar{v}) > 0$, the equilibrium (\bar{u}, \bar{v}) is locally stable if $\chi > \underline{\chi}_0$ and it is unstable if $\chi < \underline{\chi}_0$; and if $\phi(\bar{u}, \bar{v}) < 0$, the equilibrium (\bar{u}, \bar{v}) is locally stable if $\chi < \bar{\chi}_0$ and it is unstable if $\chi > \bar{\chi}_0$, where*

$$(10) \quad \underline{\chi}_0 = \min_{k \in \mathbb{N}^+} \chi_k \text{ and } \bar{\chi}_0 = \max_{k \in \mathbb{N}^+} \chi_k$$

with

$$(11) \quad \chi_k = - \frac{(d_1(\frac{k\pi}{L})^2 + \frac{a}{h}\bar{u} - \frac{b\bar{u}\bar{v}}{(\bar{u}+c)^2})d_2(\frac{k\pi}{L})^2 + \frac{bce\bar{u}\bar{v}}{(\bar{u}+c)^3}}{\frac{b\bar{u}}{\bar{u}+c}\phi(\bar{u}, \bar{v})(\frac{k\pi}{L})^2}$$

Proof. Since the proof is standard following our discussions and some straightforward calculations, we only discuss the case $\phi(\bar{u}, \bar{v}) > 0$. First of all, we see that the mode $k = 0$ is always stable since $D_0 > 0$. For each $k \in \mathbb{N}^+$, D_k is a linear function of χ which can be written as

$$D_k = \frac{b\bar{u}\phi(\bar{u}, \bar{v})}{\bar{u} + c} \left(\frac{k\pi}{L}\right)^2 (\chi - \chi_k).$$

If (\bar{u}, \bar{v}) is locally stable, then $D_k > 0$ for all $k \in \mathbb{N}^+$ which implies that χ must be bigger than the minimum of χ_k over \mathbb{N}^+ , denoted by $\underline{\chi}_0$. Similar we can easily show that (\bar{u}, \bar{v}) is unstable if $\chi < \underline{\chi}_0$. \square

We want to point out that, for each $k \in \mathbb{N}^+$, $\chi_k > 0$ if $\phi(\bar{u}, \bar{v}) < 0$ and $\chi_k < 0$ if $\phi(\bar{u}, \bar{v}) > 0$, therefore both $\underline{\chi}_0$ and $\bar{\chi}_0$ are finite numbers. Lemma 2.1 implies that prey–taxis destabilizes prey–taxis system (5) if prey–repulsion is present (due to volume–filling effect of predator species [38], or group defense of prey species [12]) which is modeled by taking $\phi(\bar{u}, \bar{v}) < 0$, while it stabilizes (5) otherwise. This lemma extends the results in [30]. If $\phi(\bar{u}, \bar{v}) = 0$, then $D_k > 0$ and (\bar{u}, \bar{v}) is locally stable. However, since we shall show that χ_k in (11) is a bifurcation value for each $k \in \mathbb{N}^+$, throughout this paper we assume that $\phi(\bar{u}, \bar{v}) \neq 0$ hence χ_k is well–defined.

2.2. Steady state bifurcation. We now study the existence of nonconstant steady state to (6). In order to apply the bifurcation theory in [5, 6, 46], we introduce the Hilbert spaces

$$\mathcal{X} = \{w \in H^2(0, L) | w'(0) = w'(L) = 0\}, \mathcal{Y} = L^2(0, L)$$

and rewrite (6) into the following equivalent abstract form

$$\mathcal{F}(u, v, \chi) = 0, (u, v, \chi) \in \mathcal{X} \times \mathcal{X} \times \mathbb{R}$$

where

$$(12) \quad \mathcal{F}(u, v, \chi) = \begin{pmatrix} d_1 u'' + u(a(1 - \frac{u}{h}) - \frac{bv}{u+c}) \\ (d_2 v' - \chi \phi(u, v)u')' + v(\frac{eu}{u+c} - d) \end{pmatrix}.$$

If (u, v) is a solution of (12) in $\mathcal{X} \times \mathcal{X}$, then it is a smooth solution of (6) thanks to the elliptic regularity theorems. We want to point out that the steady state bifurcation theory recently developed version in [46, 56] allows one to easily handle reaction–diffusion systems without reducing them into single equations; moreover the verification of necessary conditions to apply this theory, e.g. Fredholmness condition, becomes easier and more straightforward as we shall see below.

To set up the framework to apply the bifurcation theory, we collect some facts about \mathcal{F} . It is obvious that $\mathcal{F}(\bar{u}, \bar{v}, \chi) = 0, \forall \chi \in \mathbb{R}$. $\mathcal{F} : \mathcal{X} \times \mathcal{X} \times \mathbb{R} \rightarrow \mathcal{Y} \times \mathcal{Y}$ is a

continuously differentiable mapping and for any fixed $(\hat{u}, \hat{v}) \in \mathcal{X} \times \mathcal{X}$, the Fréchet derivative is

$$(13) \quad \mathcal{D}(u, v)\mathcal{F}(\hat{u}, \hat{v}, \chi) = \begin{pmatrix} d_1 u'' + \hat{u}(-\frac{a}{h} + \frac{b\hat{v}}{(\hat{u}+c)^2})u - \frac{b\hat{u}}{\hat{u}+c}v \\ d_2 v'' + \frac{ce\hat{v}}{(\hat{u}+c)^2}u + (-d + \frac{e\hat{u}}{\hat{u}+c})v + T \end{pmatrix},$$

where

$$T = -\chi(\phi(\hat{u}, \hat{v})u' + \phi_u(\hat{u}, \hat{v})\hat{u}'u + \phi_v(\hat{u}, \hat{v})\hat{u}'v)',$$

and (13) is a strictly elliptic operator. Moreover, it is easy to verify that it satisfies the Agmon's condition according to Remark 2.5 of case 2 with $N = 1$ in Shi and Wang [46]. Therefore Theorem 3.3 and Remark 3.4 in [46] imply that $\mathcal{D}_{(u,v)}\mathcal{F}(\hat{u}, \hat{v}, \chi) : \mathcal{X} \times \mathcal{X} \times \mathbb{R}^+ \rightarrow \mathcal{Y} \times \mathcal{Y}$ is Fredholm operator with zero index.

To show that bifurcation occurs at $(\bar{u}, \bar{v}, \chi_k)$, we first need implicit function theorem to fail at this point. To this end, we will show that the following condition is satisfied

$$\mathcal{N}(\mathcal{D}(u, v)\mathcal{F}(\bar{u}, \bar{v}, \chi_k)) \neq \{\mathbf{0}\}$$

or equivalently, thanks to (13), the following system has nontrivial solutions

$$(14) \quad \begin{cases} d_1 u'' + \bar{u}(-\frac{a}{h} + \frac{b\bar{v}}{(\bar{u}+c)^2})u - \frac{b\bar{u}}{\bar{u}+c}v = 0, & x \in (0, L) \\ d_2 v'' - \chi_k \phi(\bar{u}, \bar{v})u'' + \frac{ce\bar{v}}{(\bar{u}+c)^2}u = 0, & x \in (0, L) \\ u'(x) = v'(x) = 0, & x = 0, L. \end{cases}$$

Let (u, v) be a solutions to (14) with the eigen-expansions

$$u = \sum_{k=0}^{\infty} t_k \cos \frac{k\pi x}{L}, v = \sum_{k=0}^{\infty} s_k \cos \frac{k\pi x}{L},$$

where t_k and s_k are constants to be determined. Substituting these expansions into (14), multiplying the new equations by $\cos \frac{k\pi x}{L}$ and then integrating them over $(0, L)$, we collect

$$(15) \quad \begin{pmatrix} -d_1(\frac{k\pi}{L})^2 + \bar{u}(-\frac{a}{h} + \frac{b\bar{v}}{(\bar{u}+c)^2}) & -\frac{b\bar{u}}{\bar{u}+c} \\ \chi_k(\frac{k\pi}{L})^2 \phi(\bar{u}, \bar{v}) + \frac{ce\bar{v}}{(\bar{u}+c)^2} & -d_2(\frac{k\pi}{L})^2 \end{pmatrix} \begin{pmatrix} t_k \\ s_k \end{pmatrix} = \begin{pmatrix} 0 \\ 0 \end{pmatrix}.$$

It is easy to see that from (11) that the coefficient matrix in (15) is singular, therefore hence (14) has nontrivial solutions. Moreover, suppose that $\chi_k \neq \chi_j$ for $k \neq j$, then $\mathcal{N}(\mathcal{D}_{(u,v)}\mathcal{F}(\bar{u}, \bar{v}, \chi_k))$ is one-dimensional and it has span

$$\mathcal{N}(\mathcal{D}_{(u,v)}\mathcal{F}(\bar{u}, \bar{v}, \chi_k)) = \text{span}\{(\bar{u}_k, \bar{v}_k)\}_{k \in \mathbb{N}^+},$$

where

$$(16) \quad (\bar{u}_k, \bar{v}_k) = (1, Q_k) \cos \frac{k\pi x}{L}$$

with

$$(17) \quad Q_k = -\frac{d_1(\frac{k\pi}{L})^2 - \bar{u}(-\frac{a}{h} + \frac{b\bar{v}}{(\bar{u}+c)^2})}{\frac{b\bar{u}}{\bar{u}+c}}.$$

We now present the first main result of this paper which establishes nonconstant positive solutions to (6) bifurcating from (\bar{u}, \bar{v}) at $\chi = \chi_k$ for each $k \in \mathbb{N}^+$.

Theorem 2.2. *Let (\bar{u}, \bar{v}) be the positive equilibrium of (6) giving by (2) and assume that condition (3) holds. Suppose that $\phi(\bar{u}, \bar{v}) \neq 0$ and for all different positive integers $k, j \in \mathbb{N}^+$*

$$(18) \quad d_1 d_2 k^2 j^2 \left(\frac{\pi}{L}\right)^4 \neq \frac{bce\bar{u}\bar{v}}{(\bar{u}+c)^3}, k \neq j.$$

Then for each $k \in \mathbb{N}^+$, there exists a small positive constant δ such that (6) admits nonconstant positive solutions $(u_k(s, x), v_k(s, x), \chi_k(s)) \in \mathcal{X} \times \mathcal{X} \times \mathbb{R}^+$ for $s \in (-\delta, \delta)$ with $(u_k(0, x), v_k(0, x), \chi_k(0)) = (\bar{u}, \bar{v}, \chi_k)$, where χ_k is given by (11); moreover the solutions are continuously differentiable functions of s and have the following asymptotic expansions

$$(19) \quad (u_k(s, x), v_k(s, x)) = (\bar{u}, \bar{v}) + s(1, Q_k) \cos \frac{k\pi x}{L} + s^2(\Phi, \Psi), s \in (-\delta, \delta),$$

where (Φ, Ψ) is an element in any complement \mathcal{Z} of $\text{span}\{(\bar{u}_k, \bar{v}_k)\}_{k \in \mathbb{N}^+}$ given by

$$(20) \quad \mathcal{Z} = \left\{ (\Phi, \Psi) \in \mathcal{X} \times \mathcal{X} \mid \int_0^L (\Phi + Q_k \Psi) \cos \frac{k\pi x}{L} dx = 0 \right\};$$

furthermore all nontrivial solutions of (6) around $(\bar{u}, \bar{v}, \chi_k)$ must stay on the curve $\Gamma_k(s) = (u_k(s, x), v_k(s, x), \chi_k(s))$, $s \in (-\delta, \delta)$.

Proof. Our results follow from Theorem 1.7 of Crandall and Rabinowitz [5] once we prove the following transversality condition

$$(21) \quad \frac{d}{d\chi} (D_{(u,v)} \mathcal{F}(\bar{u}, \bar{v}, \chi)) (\bar{u}_k, \bar{v}_k)|_{\chi=\chi_k} \notin \mathcal{R}(D_{(u,v)} \mathcal{F}(\bar{u}, \bar{v}, \chi_k)),$$

where (\bar{u}_k, \bar{v}_k) is given in (16) and $\mathcal{R}(\cdot)$ denotes range of the operator. We argue by contradiction and assume that (21) fails, then there exist a nontrivial pair (\tilde{u}, \tilde{v}) to the following problem

$$(22) \quad \begin{cases} d_1 \tilde{u}'' + \bar{u} \left(-\frac{a}{h} + \frac{b\bar{v}}{(\bar{u}+c)^2} \right) \tilde{u} - \frac{b\bar{u}}{\bar{u}+c} \tilde{v} = 0, & x \in (0, L), \\ d_2 \tilde{v}'' - \chi_k \phi(\bar{u}, \bar{v}) \tilde{u}'' + \frac{ce\bar{v}}{(\bar{u}+c)^2} \tilde{u} = \left(\frac{k\pi}{L} \right)^2 \phi(\bar{u}, \bar{v}) \cos \frac{k\pi x}{L}, & x \in (0, L). \end{cases}$$

Multiplying (22) by $\cos \frac{k\pi x}{L}$ and integrating them over $(0, L)$ by parts, we have

$$\begin{aligned} & \begin{pmatrix} -d_1 \left(\frac{k\pi}{L} \right)^2 + \bar{u} \left(-\frac{a}{h} + \frac{b\bar{v}}{(\bar{u}+c)^2} \right) & -\frac{b\bar{u}}{\bar{u}+c} \\ \chi_k \left(\frac{k\pi}{L} \right)^2 \phi(\bar{u}, \bar{v}) + \frac{ce\bar{v}}{(\bar{u}+c)^2} & -d_2 \left(\frac{k\pi}{L} \right)^2 \end{pmatrix} \begin{pmatrix} \int_0^L \tilde{u} \cos \frac{k\pi x}{L} dx \\ \int_0^L \tilde{v} \cos \frac{k\pi x}{L} dx \end{pmatrix} \\ & = \begin{pmatrix} 0 \\ \frac{(k\pi)^2}{2L} \phi(\bar{u}, \bar{v}) \end{pmatrix}. \end{aligned}$$

The coefficient matrix is singular thanks to (11), therefore (22) has no solutions and this proves the transversality condition (21). Moreover, (18) implies that $\chi_i \neq \chi_j$, $\forall i \neq j$, hence the Frechet derivative in (21) has simple eigen-value. Then χ_k is a bifurcation value and the statements in Theorem 2.2 follow from Theorem 1.7 and Theorem 1.18 in [5]. The proof of Theorem 2.2 is complete. \square

Theorem 2.2 establishes the existence and asymptotic expansions of positive solutions to (6) on each local branch $\Gamma_k(s)$ when χ is around χ_k . In the qualitative studies of prey-taxis system (5), it is important to study the global continuum of its steady state bifurcation branches since positive solutions may exhibit striking structures in the limit of bifurcation parameter. According to the global bifurcation theory for Fredholm operators [41, 46] (see [56] for a user-friendly review e.g.), the continuum of $\Gamma_k(s)$, denoted by \mathcal{C} , satisfies one of the following three alternatives:

- (a). it is not compact in $\mathcal{X} \times \mathcal{X} \times \mathbb{R}^+$;
- (b). it contains a point $(\bar{u}, \bar{v}, \chi^*)$ with $\chi^* \neq \chi_k$;
- (c). it contains a point $(\bar{u} + u^*, \bar{v} + v^*)$ with $\mathbf{0} \neq (u^*, v^*) \in \mathcal{Z}$ defined by (20).

In [3, 56], a novel approach has been developed, based on maximum principles and topology argument, to obtain global bifurcation for a class of chemotaxis steady

state system without cellular growth in 1D. It is showed cases (b) and (c) can not occur for the first bifurcation branch and its continuum must (eventually) extend to infinity in the positive direction in the axis of bifurcation parameter. Then they were able to show that this class of chemotaxis system develops various interesting patterns such as boundary spikes, transition layers, etc in the limit of large chemotaxis rate. These patterns can be used to model the celebrated cellular aggregation phenomenon in chemotaxis. See the applications of this approach in shadow systems [50, 51].

In [55], the authors performed local bifurcation analysis for (1) with $\phi(u, v) \equiv v$ over high space dimensions. Global bifurcation result is also provided there which states that case (b) and case (c) can not occur for each local bifurcation branch and the continuum of Γ_k must extend to infinity in the positive direction of χ -axis for each $k \in \mathbb{N}^+$. Though it is not the goal of our work to agree with or disagree with these statements with a rigorous proof, we find that very recently in [33], Ma and Wang obtained global bifurcation of chemotaxis model with logistic cellular growth in one-dimensional space, where they apply a reflective and periodic extension method as in [18]. This work extends that in [56] and provides a foundation for the qualitative analysis of positive steady state to logistic chemotaxis models in the limit of large chemotaxis rate. We surmise that their approach carries over for (6) and detailed arguments are out of scope of this paper.

3. Stability analysis of bifurcating solutions

We proceed to study the local stability of the bifurcation branches $\Gamma_k(s)$ to (6) obtained in Theorem 2.2, with the bifurcating solution $(u_k(s, x), v_k(s, x), \chi_k(s))$ viewed as an equilibrium to the time-dependent system of (6). \mathcal{F} is C^4 -smooth in s if ϕ is C^4 , therefore, according to Theorem 1.18 in [5], we have the following asymptotic expansions of $(u_k(s, x), v_k(s, x), \chi_k(s))$

$$(23) \quad \begin{cases} u_k(s, x) = \bar{u} + s \cos \frac{k\pi x}{L} + s^2 \varphi_1 + s^3 \varphi_2 + \mathcal{O}(s^4), \\ v_k(s, x) = \bar{v} + s Q_k \cos \frac{k\pi x}{L} + s^2 \psi_1 + s^3 \psi_2 + \mathcal{O}(s^4), \\ \chi = \chi_k + s \mathcal{K}_1 + s^2 \mathcal{K}_2 + o(s^2), \end{cases}$$

where \mathcal{O} -terms are taken in \mathcal{X} -topology; $\mathcal{K}_1, \mathcal{K}_2$ are constants to be determined and we have skipped index k without confusing the reader; moreover (φ_i, ψ_i) , $i = 1, 2$, are in the closed complement of the null space $\mathcal{N}(D_{(u,v)}\mathcal{F}(\bar{u}, \bar{v}, \chi_k))$, that being said

$$(24) \quad (\varphi_i, \psi_i) \in \mathcal{X} \times \mathcal{X} \text{ and } \int_0^L \varphi_i \bar{u}_k + \psi_i \bar{v}_k dx = 0, i = 1, 2,$$

where (\bar{u}_k, \bar{v}_k) is given by (16).

3.1. Pitch-fork bifurcation. We first show that $\Gamma_k(s)$ is pitch-fork by proving $\mathcal{K}_1 = 0$. Here and in the sequel we denote $\bar{\phi} = \phi(\bar{u}, \bar{v}), \bar{\phi}_u = \frac{\partial \phi(\bar{u}, \bar{v})}{\partial u}, \dots$ etc. We

have from Taylor's expansions that

$$\begin{aligned}
\phi(u_k, v_k) &= \bar{\phi} + s(\bar{\phi}_u + \bar{\phi}_v Q_k) \cos \frac{k\pi x}{L} \\
&\quad + s^2 \left(\bar{\phi}_u \varphi_1 + \bar{\phi}_v \psi_1 + \frac{1}{2}(\bar{\phi}_{uu} + 2\bar{\phi}_{uv} Q_k + \bar{\phi}_{vv} Q_k^2) \cos^2 \frac{k\pi x}{L} \right) \\
&\quad + s^3 \left(\bar{\phi}_u \varphi_2 + \bar{\phi}_v \psi_2 + (\bar{\phi}_{uu} + \bar{\phi}_{uv} Q_k) \varphi_1 \cos \frac{k\pi x}{L} \right. \\
&\quad \left. + (\bar{\phi}_{uv} + \bar{\phi}_{vv} Q_k) \psi_1 \cos \frac{k\pi x}{L} \right. \\
(25) \quad &\quad \left. + \frac{1}{6}(\bar{\phi}_{uuu} + 3\bar{\phi}_{uuv} Q_k + 3\bar{\phi}_{uvv} Q_k^2 + \bar{\phi}_{vvv} Q_k^3) \cos^3 \frac{k\pi x}{L} \right) + \mathcal{O}(s^4).
\end{aligned}$$

Substituting (23) and (25) into the first equation of (6), and then collecting the s^2 -terms there we have

$$(26) \quad \begin{cases} d_1 \varphi_1'' + \bar{u} \left(-\frac{a}{h} + \frac{b\bar{v}}{(\bar{u}+c)^2} \right) \varphi_1 - \frac{b\bar{u}}{\bar{u}+c} \psi_1 \\ = \left(-\frac{bc\bar{v}}{(\bar{u}+c)^3} + \frac{a}{h} + \frac{bcQ_k}{(\bar{u}+c)^2} \right) \cos^2 \frac{k\pi x}{L}, & \in (0, L), \\ d_2 \psi_1'' + \frac{ce\bar{v}}{(\bar{u}+c)^2} \varphi_1 + \left(\frac{k\pi}{L} \right)^2 \bar{\phi} \cos \frac{k\pi x}{L} \mathcal{K}_1 \\ = \chi_k (\bar{\phi} \varphi_1'' + (\bar{\phi}_u + \bar{\phi}_v Q_k) (\cos \frac{k\pi x}{L} (\cos \frac{k\pi x}{L})'))' \\ + \left(\frac{ce\bar{v}}{(\bar{u}+c)^3} - \frac{ceQ_k}{(\bar{u}+c)^2} \right) \cos^2 \frac{k\pi x}{L}, & x \in (0, L), \\ \varphi_1'(x) = \psi_1'(x) = 0, & x = 0, L. \end{cases}$$

Multiplying the first and second equation of (26) by $\cos \frac{k\pi x}{L}$ and then integrating them over $(0, L)$ by parts, we collect

$$(27) \quad \frac{b\bar{u}}{\bar{u}+c} \int_0^L \psi_1 \cos \frac{k\pi x}{L} dx + \left(d_1 \left(\frac{k\pi}{L} \right)^2 - \bar{u} \left(-\frac{a}{h} + \frac{b\bar{v}}{(\bar{u}+c)^2} \right) \right) \int_0^L \varphi_1 \cos \frac{k\pi x}{L} dx = 0$$

and

$$\begin{aligned}
(28) \quad \frac{(k\pi)^2 \bar{\phi} \mathcal{K}_1}{2L} &= - \left(\frac{ce\bar{v}}{(\bar{u}+c)^2} + \chi_k \bar{\phi} \left(\frac{k\pi}{L} \right)^2 \right) \int_0^L \varphi_1 \cos \frac{k\pi x}{L} dx \\
&\quad + d_2 \left(\frac{k\pi}{L} \right)^2 \int_0^L \psi_1 \cos \frac{k\pi x}{L} dx.
\end{aligned}$$

Solving (27) with (24) gives us

$$(1 + Q_k^2) \int_0^L \varphi_1 \cos \frac{k\pi x}{L} dx = 0,$$

then we have that

$$\int_0^L \psi_1 \cos \frac{k\pi x}{L} dx = \int_0^L \varphi_1 \cos \frac{k\pi x}{L} dx = 0, \quad \forall k \in \mathbb{N}^+.$$

Finally it follows from (28) that $\mathcal{K}_1 = 0$, hence the bifurcation branch $\Gamma_k(s)$ around χ_k is of pitch-fork type, i.e., one-sided. As we shall see in the coming analysis, the sign of \mathcal{K}_2 determines the branch direction hence the stability of $(u_k(s, x), v_k(s, x), \chi_k(s))$. In order to evaluate, one equates the s^3 -terms in (23) and collect a system of ϕ_2, ψ_2 and \mathcal{K}_2 similar as (26). By the same calculations that lead to $\mathcal{K}_1 = 0$, we will be able to express \mathcal{K}_2 in terms of system parameters. Since the computations are straightforward but very involved, we skip them here.

3.2. Stability results. In light of the fact that $\mathcal{K}_1 = 0$ in (23) for each $k \in \mathbb{N}^+$, here we give another main result of this paper about the stability of the bifurcating solutions on $\Gamma_k(s)$ around $(\bar{u}, \bar{v}, \chi_k)$. Here by the stability of $\Gamma_k(s)$ we mean that of the bifurcating solution on this branch viewed as an equilibrium to (5). Our stability analysis of the bifurcating solutions is based on Theorem 1.16 in [6] and we now present the following results.

Theorem 3.1. *Assume that all the conditions in Theorem 2.2 hold and $\phi(\bar{u}, \bar{v}) \neq 0$. Then the following statements hold:*

(i). *If $\phi(\bar{u}, \bar{v}) > 0$. Suppose that $\chi_{k_0} = \min_{k \in \mathbb{N}^+} \chi_k$, then for each $k \neq k_0$, $\Gamma_k(s)$, $s \in (-\delta, \delta)$ is always unstable; $\Gamma_{k_0}(s)$, $s \in (-\delta, \delta)$ is stable if $\mathcal{K}_2 > 0$ and it is unstable if $\mathcal{K}_2 < 0$.*

(ii). *If $\phi(\bar{u}, \bar{v}) < 0$. Suppose that $\chi_{k_1} = \max_{k \in \mathbb{N}^+} \chi_k$, then for each $k \neq k_1$, $\Gamma_k(s)$, $s \in (-\delta, \delta)$ is always unstable; $\Gamma_{k_1}(s)$, $s \in (-\delta, \delta)$ is stable if $\mathcal{K}_2 < 0$ and it is unstable if $\mathcal{K}_2 > 0$.*

Proof. We shall only prove part (i) and part (ii) can be proved by the same arguments. Linearize (6) around $(u_k(s, x), v_k(s, x), \chi_k(s))$, then the branch $\Gamma_k(s)$ will be asymptotically stable if the real part of any eigenvalue λ of the following problem is negative:

$$(29) \quad \mathcal{D}_{(u,v)} \mathcal{F}(u_k(s, x), v_k(s, x), \chi_k(s))(u, v) = \lambda(u, v), \quad (u, v) \in \mathcal{X} \times \mathcal{X}.$$

According to Corollary 1.13 in [6], there exist an interval I containing χ_k and C^1 -smooth functions $(\chi, s) : I \times (-\delta, \delta) \rightarrow (\mu(\chi), \lambda(s))$ with $\lambda(0) = 0$ and $\mu(\chi_k) = 0$ such that, $\lambda(s)$ is an eigenvalue of (29) and $\mu(\chi)$ is an eigenvalue of the following eigenvalue problem

$$\mathcal{D}_{(u,v)} \mathcal{F}(\bar{u}, \bar{v}, \chi)(u, v) = \mu(u, v), \quad (u, v, \chi) \in \mathcal{X} \times \mathcal{X} \times I$$

or equivalently the following eigenvalue problem

$$(30) \quad \begin{cases} d_1 u'' + \bar{u} \left(-\frac{a}{h} + \frac{b\bar{v}}{(\bar{u}+c)^2} \right) u - \frac{b\bar{u}}{\bar{u}+c} v = \mu(\chi) u, & x \in (0, L), \\ d_2 v'' - \chi \phi(\bar{u}, \bar{v}) u'' + \frac{ce\bar{v}}{(\bar{u}+c)^2} u = \mu(\chi) v, & x \in (0, L), \\ u'(x) = v'(x) = 0, & x = 0, L. \end{cases}$$

Moreover, $\lambda(s)$ is the only eigenvalue of (29) in any fixed neighbourhood of the origin of the complex plane and $\mu(\chi)$ is the only eigenvalue of (30) around χ_k . Furthermore the eigenfunction of (30) can be represented by $(u(\chi, x), v(\chi, x))$, which depends on χ smoothly and is uniquely determined by $(u(\chi_k, x), v(\chi_k, x)) = \left(\cos \frac{k\pi x}{L}, Q_k \cos \frac{k\pi x}{L} \right)$ and $(u(\chi, x), v(\chi, x)) = \left(\cos \frac{k\pi x}{L}, Q_k \cos \frac{k\pi x}{L} \right) \in \mathcal{Z}$, where Q_k and \mathcal{Z} are defined by (17) and (20) respectively.

To prove the instability of $\Gamma_k(s)$ around $(\bar{u}, \bar{v}, \chi_k)$ for each $k \neq k_0$, we first study the limit of (29) as $s \rightarrow 0$, or equivalently the following eigenvalue problem

$$(31) \quad \begin{cases} d_1 u'' + \bar{u} \left(-\frac{a}{h} + \frac{b\bar{v}}{(\bar{u}+c)^2} \right) u - \frac{b\bar{u}}{\bar{u}+c} v = \lambda(0) u, & x \in (0, L), \\ d_2 v'' - \chi_k \phi(\bar{u}, \bar{v}) u'' + \frac{ce\bar{v}}{(\bar{u}+c)^2} u = \lambda(0) v, & x \in (0, L), \\ u'(x) = v'(x) = 0, & x = 0, L. \end{cases}$$

Testing (31) by $\cos \frac{k\pi x}{L}$ over $(0, L)$ by parts gives rise to

$$\begin{pmatrix} -d_1(\frac{k\pi}{L})^2 + \bar{u}(-\frac{a}{h} + \frac{b\bar{v}}{(\bar{u}+c)^2}) - \lambda(0) & -\frac{b\bar{u}}{\bar{u}+c} \\ \chi_k(\frac{k\pi}{L})^2\phi(\bar{u}, \bar{v}) + \frac{ce\bar{v}}{(\bar{u}+c)^2} & -d_2(\frac{k\pi}{L})^2 - \lambda(0) \end{pmatrix} \\ \times \begin{pmatrix} \int_0^L u \cos \frac{k\pi x}{L} dx \\ \int_0^L v \cos \frac{k\pi x}{L} dx \end{pmatrix} = \begin{pmatrix} 0 \\ 0 \end{pmatrix},$$

therefore $\lambda(0)$ is an eigenvalue of (31) if and only if $p_k(\lambda_0) = \lambda_0^2 - T_k\lambda_0 + D_k$, where T_k and $D_k = D_k(\chi_k)$ are the same as given in (8) with $\chi = \chi_k$. It is easy to see that for any $k \neq k_0$ $T_k > 0$ and $D_k(\chi_k) > 0$ from the definition of k_0 , therefore $p_k(\lambda) = 0$ has a root $\lambda(0) > 0$ which is also an eigenvalue of (31). From the standard eigenvalue perturbation theory in [20], (29) always has a positive root in a small neighborhood of the origin of the complex plane if $k \neq k_0$. This shows that for each $k \neq k_0$, $\Gamma_k(s)$ is unstable for $s \in (-\delta, \delta)$. We want to point out that 0 is a simple eigenvalue of (31) since $\chi_k \neq \chi_j$ for $k \neq j$.

Now we proceed to study the stability of the nonconstant solutions $(u_{k_0}(s, x), v_{k_0}(s, x))$ on branch $\Gamma_k(s)$, $s \in (-\delta, \delta)$. According to the analysis above, we see that the characteristic polynomial $p(\lambda_0)$ hence (30) with $k = k_0$ has one negative eigenvalue and a zero eigenvalue. Therefore we only need to study the property of this zero eigenvalue around $s = 0$ which will be denoted by $\lambda(s)$ as above without confusing our reader. In particular, $(u_{k_0}(s, x), v_{k_0}(s, x))$ is asymptotically stable if $\lambda(s) < 0$ and it is unstable if $\lambda(s) > 0$. Taking $s = 0$, following the same analysis that leads to (21), we have that $\lambda = 0$ is a simple eigenvalue of $\mathcal{D}_{(u,v)}\mathcal{F}(\bar{u}, \bar{v}, \chi_k)$ and the eigenspace is $\mathcal{N}(\mathcal{D}_{(u,v)}\mathcal{F}(\bar{u}, \bar{v}, \chi_k)) = \{(1, Q_k) \cos \frac{k\pi x}{L}\}$ and $(1, Q_k) \cos \frac{k\pi x}{L}$ is not in the range of this operator.

Differentiating (30) with respect to χ and taking $\chi = \chi_{k_0}$ give us

$$(32) \quad \begin{cases} d_1 \dot{u}'' + \bar{u}(-\frac{a}{h} + \frac{b\bar{v}}{(\bar{u}+c)^2})\dot{u} - \frac{b\bar{u}}{\bar{u}+c}\dot{v} = \dot{\mu}(\chi_{k_0}) \cos \frac{k_0\pi x}{L}, & x \in (0, L), \\ d_2 \dot{v}'' - \chi_{k_0}\phi(\bar{u}, \bar{v}) \cos'' \frac{k_0\pi x}{L} - \phi(\bar{u}, \bar{v})\dot{u}'' + \frac{ce\bar{v}}{(\bar{u}+c)^2}\dot{u} = \dot{\mu}(\chi_{k_0}) \cos \frac{k_0\pi x}{L}, & x \in (0, L), \\ \dot{u}'(x) = \dot{v}'(x) = 0, & x = 0, L, \end{cases}$$

where the dot-notation $\dot{\cdot}$ in (32) denotes the differentiation with respect to χ evaluated at $\chi = \chi_{k_0}$ and in particular $\dot{u} = \frac{\partial u(\chi, x)}{\partial \chi}|_{\chi=\chi_{k_0}}$, $\dot{v} = \frac{\partial v(\chi, x)}{\partial \chi}|_{\chi=\chi_{k_0}}$.

By Theorem 1.16 in [6], the eigenvalue $\lambda(s)$ of (29) and the function $-s\chi'_{k_0}(s)\dot{\mu}(\chi_{k_0})$ have the same zeros and the same sign near $s = 0$ if $\lambda(s) \neq 0$, and

$$(33) \quad \lim_{s \rightarrow 0, \lambda(s) \neq 0} \frac{-s\chi'_{k_0}(s)\dot{\mu}(\chi_{k_0})}{\lambda(s)} = 1.$$

On the other hand, multiplying both equations in (32) by $\cos \frac{k_0\pi x}{L}$ and integrating them over $(0, L)$ by parts, we arrive at the following system

$$\begin{pmatrix} -d_1(\frac{k_0\pi}{L})^2 + \bar{u}(-\frac{a}{h} + \frac{b\bar{v}}{(\bar{u}+c)^2}) & -\frac{b\bar{u}}{\bar{u}+c} \\ \chi_{k_0}(\frac{k_0\pi}{L})^2\phi(\bar{u}, \bar{v}) + \frac{ce\bar{v}}{(\bar{u}+c)^2} & -d_2(\frac{k_0\pi}{L})^2 \end{pmatrix} \begin{pmatrix} \int_0^L \dot{u} \cos \frac{k_0\pi x}{L} dx \\ \int_0^L \dot{v} \cos \frac{k_0\pi x}{L} dx \end{pmatrix} \\ = \begin{pmatrix} \dot{\mu}(\chi_{k_0})\frac{L}{2} \\ (\dot{\mu}(\chi_{k_0})Q_{k_0} - \phi(\bar{u}, \bar{v}))(\frac{k_0\pi}{L})^2\frac{L}{2} \end{pmatrix}$$

We see from (33) that the coefficient matrix is singular, therefore if the algebraic system is solvable, we must have that $\frac{d_2(\frac{k_0\pi}{L})^2}{b\bar{u}/(\bar{u}+c)} = \frac{\dot{\mu}(\chi_{k_0})Q_{k_0} - \phi(\bar{u}, \bar{v})(\frac{k_0\pi}{L})^2}{\dot{\mu}(\chi_{k_0})}$, which together with (3) implies that $\text{sgn}(\dot{\mu}(\chi_{k_0})) = -\text{sgn}(\phi(\bar{u}, \bar{v}))$, therefore $\text{sgn}(\lambda(s)) =$

$\text{sgn}(\phi(\bar{u}, \bar{v})\mathcal{K}_2)$ in light of (33) since $\mathcal{K}_1 = 0$. Therefore, the sign of \mathcal{K}_2 determines that of $\lambda(s)$ hence the stability of the bifurcating branches. This completes the proof of Theorem 3.1. \square

The local bifurcation branches described in Theorem 3.1 are schematically presented in Figure 1. Theorem 3.1 inserts that, among the infinitely many local

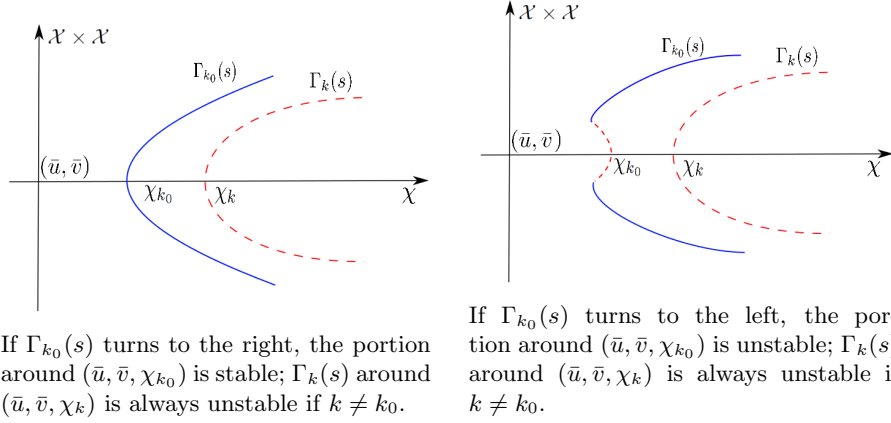


FIGURE 1. Bifurcation diagrams when case (i) in Theorem 3.1 occurs. The stable bifurcation curve is plotted in solid lines and the unstable bifurcation curve is plotted in dashed lines. The bifurcation curve is of pitch-fork type, i.e., being one-sided.

bifurcation branches, the only stable branch must be the portion of the left-most one that turns to the right if $\phi(\bar{u}, \bar{v}) > 0$ or the portion of the right-most branch that turns to the left if $\phi(\bar{u}, \bar{v}) < 0$. Moreover, according to Lemma 2.1, (\bar{u}, \bar{v}) loses its stability to nontrivial steady states of (6) that has a spatial pattern $\cos \frac{k_0 \pi x}{L}$ or $\cos \frac{k_1 \pi x}{L}$ when $\phi(\bar{u}, \bar{v}) > 0$ or $\phi(\bar{u}, \bar{v}) < 0$ respectively.

It is necessary to point out that, though Theorem 3.1 provides a complete understanding on the local branches, we do not know much about the global behaviors of the stationary system (6) or the time-dependent system (5). Indeed (5) has extremely rich and complicated dynamics such as the merging and emerging of spikes or time-periodic spatial patterns. See our numerical simulations in Figures 5 and Figure 6 for example, where χ is chosen to be far away from χ_{k_0} or χ_{k_1} .

In general, it is impossible to determine at which k that χ_k achieves its minimum or maximum as in (10). When the interval length L is sufficiently small, we calculate in (11) that $\chi_k \approx -\frac{d_1 d_2 (\frac{k\pi}{L})^2}{\frac{b\bar{u}}{\bar{u}+c} \phi(\bar{u}, \bar{v})}$, therefore $\min \chi_k$ or $\max \chi_k$ is achieved at $k = 1$ either $\phi(\bar{u}, \bar{v}) > 0$ or $\phi(\bar{u}, \bar{v}) < 0$, this indicates that when the interval is small, (\bar{u}, \bar{v}) loses its stability to $\cos \frac{\pi x}{L}$ which is spatially monotone; moreover larger intervals supports larger wavemode and more interior spikes. See Figure 3 for numerical simulations which support this conclusion.

4. Numerical simulations

In this section, we perform some numerical studies on the formation of spatial patterns in system (5). We choose the potential function to be $\phi(u, v) = uv(M - v)$ for some positive constant M to be selected in each simulation. Here M measures the threshold value of volume-filling effect above which predators escape the region

with their over-crowding focal species. Throughout this section we choose the initial data to be $(u_0, v_0) = (\bar{u}, \bar{v}) + 0.01 \cos 2.4\pi x$, which are small perturbations of the homogenous equilibrium (\bar{u}, \bar{v}) given by (2), then we investigate several sets of system parameters to study the regime under which small perturbed inhomogeneous data can develop into stationary or time-periodic solutions with spatial patterns. In particular, the numerics support our theoretical findings on the existence and stability of the bifurcating solutions established in Theorem 2.2 and Theorem 3.1.

In Figure 2, we show the formation and stabilization of stationary patterns of system (5) developed from steady state bifurcation over $\Omega = (0, 6)$. System parameters are chosen to be $d_1 = 0.5$, $d_2 = 1$, $a = 2.5$, $b = 1$, $c = 0.2$, $d = 3$, $e = 4.5$ and $h = 0.6$ therefore the unique positive equilibrium is $(\bar{u}, \bar{v}) = (0.4, 0.5)$. The volume-filling threshold value in ϕ is taken $M = 0.1$. We calculate (14) to find that $\min_{k \in \mathbb{N}^+} \chi_k = \chi_2 \approx 18.145$, therefore $k_0 = 2$ is the stable wave number and $\cos \frac{2\pi x}{6}$ is the stable wave mode to which the equilibrium $(\bar{u}, \bar{v}) = (0.4, 0.5)$ loses its stability, despite that the initial data have spatial mode $\cos 2.4\pi x$. This supports our stability analysis of the bifurcating solutions obtained in Theorem 2.2.

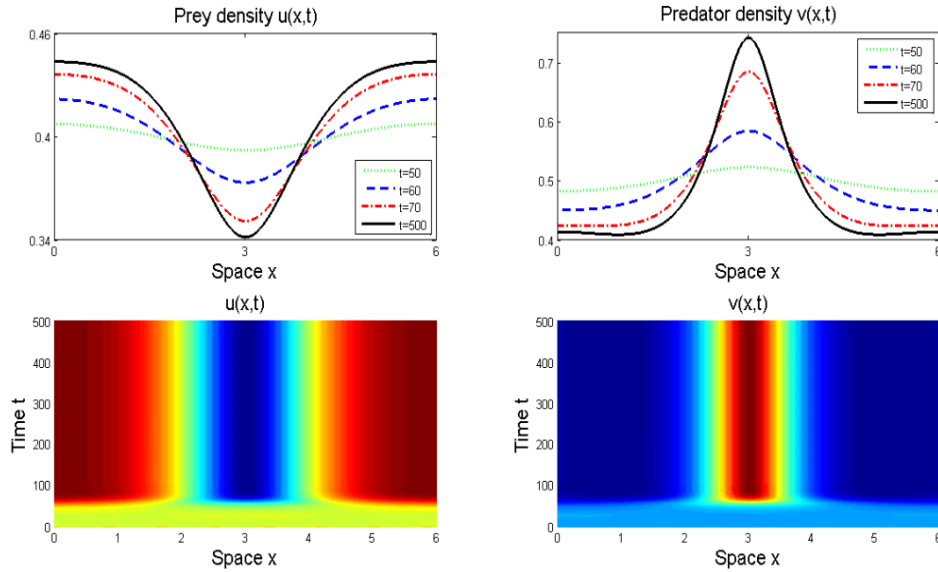


FIGURE 2. Formation of stationary stable patterns of (5) over $\Omega = (0, 6)$ from initial data (u_0, v_0) being small perturbations from (\bar{u}, \bar{v}) with spatial mode $\cos 2.4\pi x$. System parameters are chosen $d_1 = 0.5$, $d_2 = 1$, $a = 2.5$, $b = 1$, $c = 0.2$, $d = 3$, $e = 4.5$, $h = 0.6$ and $M = 0.1$. Prey-taxis is chosen to be $\chi = 20$ around the critical bifurcation value $\chi_2 = 18.145$.

In Figure 3, we examine the effect of interval length on the variation of patterns in (5) when prey-taxis rate χ is around the critical bifurcation value. System parameters and initial data are taken to be the same as those for Figure 2. We select interval length to be $L = 8, 11, 13$ and 16 in each graph, which corresponds to the critical bifurcation values $\chi_3 \approx 18.0412$, $\chi_4 \approx 18.0164$, $\chi_5 \approx 18.0892$ and $\chi_6 \approx 18.0412$ in each plot from the left to the right. Therefore according to Theorem 2.2, (\bar{u}, \bar{v}) loses its stability to the stable wave mode $\cos \frac{3\pi x}{8}$, $\cos \frac{4\pi x}{11}$, $\cos \frac{5\pi x}{13}$ and $\cos \frac{6\pi x}{16}$ respectively and this is verified numerically in Figure 3. We observe that

a larger interval supports higher wave number than a smaller interval hence stable patterns with more aggregates. Indeed, by periodically reflecting and extending (5) from $(0, L)$ to $(0, 2L)$, one can expect similar dynamics between the same system over these two intervals, e.g, as intuitively observed in the plots with $L = 8$ to $L = 16$.

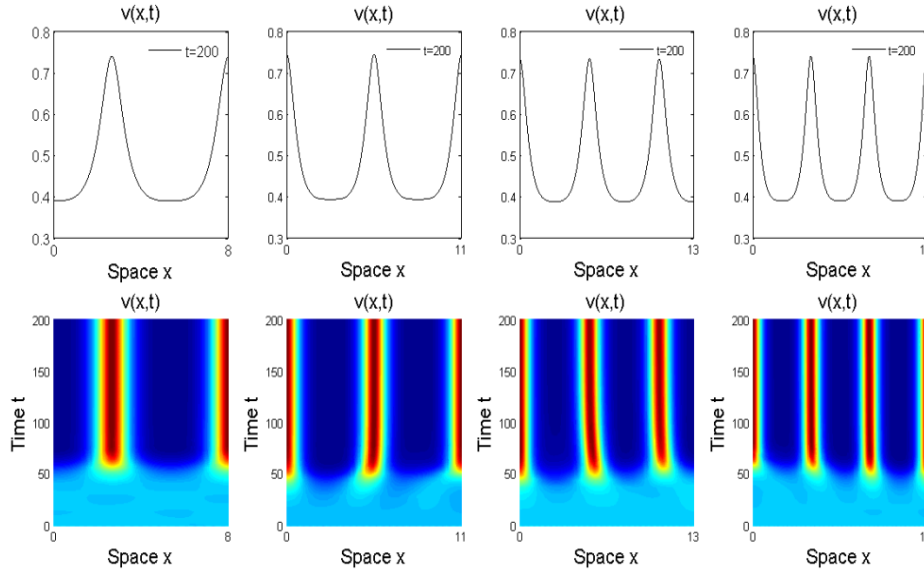


FIGURE 3. Effect of interval size on the formation of nontrivial steady states from small perturbations of (\bar{u}, \bar{v}) . System parameters and initial data in (5) are the same as in Figure 2. These plots agree very well with the wave mode selection mechanism implied by Theorem 3.1. We observe that large intervals support more aggregates than small intervals.

Figure 4 provides insights on how a large prey-taxis rate χ effects pattern formations in (5) qualitatively. All system parameters are chosen to be the same as in Figure 2 except that the domain size L changes to 7 and the prey-taxis rate χ is larger than the minimum bifurcation value $\chi_3 \approx 18.579$. $\phi(\bar{u}, \bar{v}) < 0$ since $M < \bar{v}$ therefore a larger prey-taxis rate χ benefits the spatial heterogeneity and aggregation of population species in (5). Our simulations suggest that species population densities develop into spiky functions when χ is large.

As the prey-taxis rate χ increases, sometimes we observe spatially inhomogeneous time-periodic phenomena presented in Figure 5. We choose $\chi = 0.089$, which is bigger than the critical bifurcation value $\chi_6 = 0.072$. And we can also observe that the wave mode number is $k = 6$ even in time-periodic pattern, and the rigorous analysis is out of our scope of our paper. It is necessary to point out that spatial-temporal periodic patterns have been observed in chemotaxis models with cellular growths [8, 39, 53, 54], as well as for two-predator and one-prey systems with prey-taxis [49].

Finally, we present Figure 6 with the formation of stationary patterning process though merging and emerging or spikes in (5). Here merging refers to two peaks that collide and form a single peak while emerging refers to a new peak that appears from between two peaks, as shown at time $t \approx 120s$.

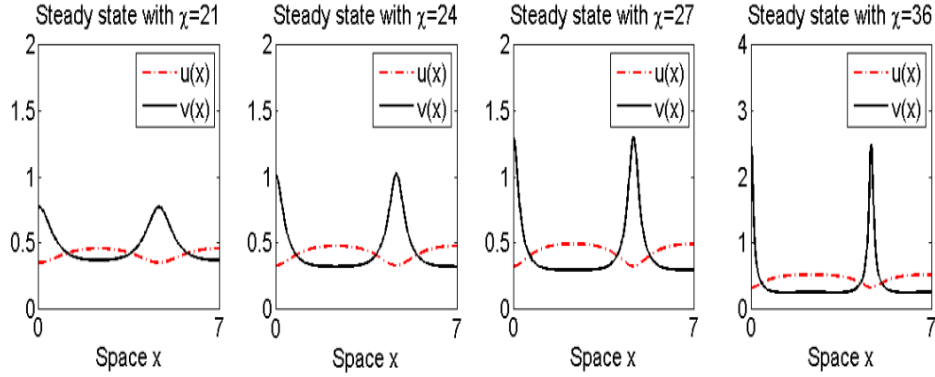


FIGURE 4. Formation of nonconstant positive steady states to (5) over $\Omega = (0, 7)$ when prey-taxis χ is chosen to be larger than the critical bifurcation value $\chi_3 \approx 18.579$. Initial data and system parameters are chosen to be the same as in Figure 2 except that $L = 7$ and $\chi = 21, 24, 27$ and 36 in each plot from left to right.

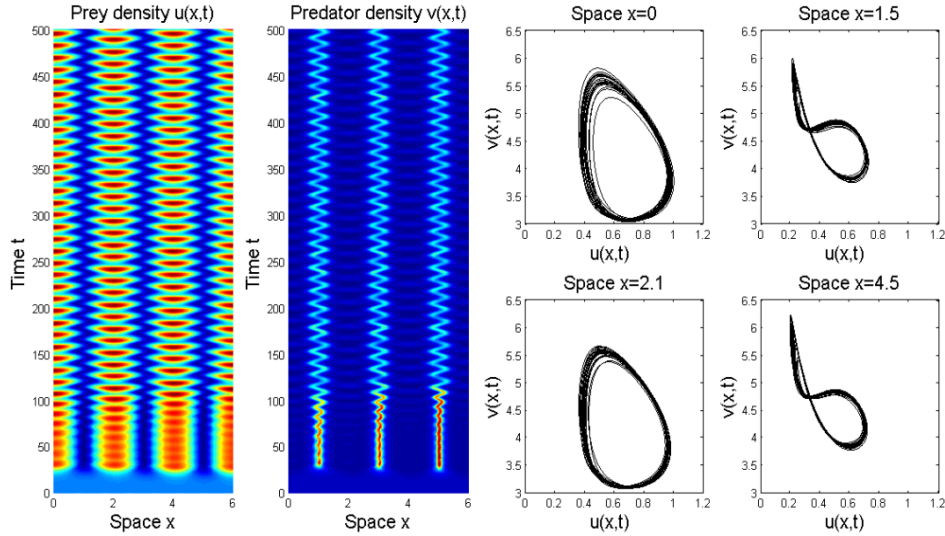


FIGURE 5. Regular time-periodic patterning in (5) from (\bar{u}, \bar{v}) over $\Omega = (0, 6)$. Subplots in lines show the prey-predator phase plane at the each space location for time $t \in (200, 500)$. System parameters are chosen $d_1 = 0.1$, $d_2 = 0.1$, $a = 2.5$, $b = 1$, $c = 2$, $d = 0.5$, $e = 4$, $h = 2.5$ and $\chi = 0.089$, $M = 0.7$. These simulations demonstrate the sustained coexistence and spatial-temporal oscillations of prey and predator species over the habitat.

Acknowledgements

L.X. is supported by Guangdong Natural Science Foundation (2015A030313623) and Guangdong Training Program for Young College Teachers (YQ2015077). Both

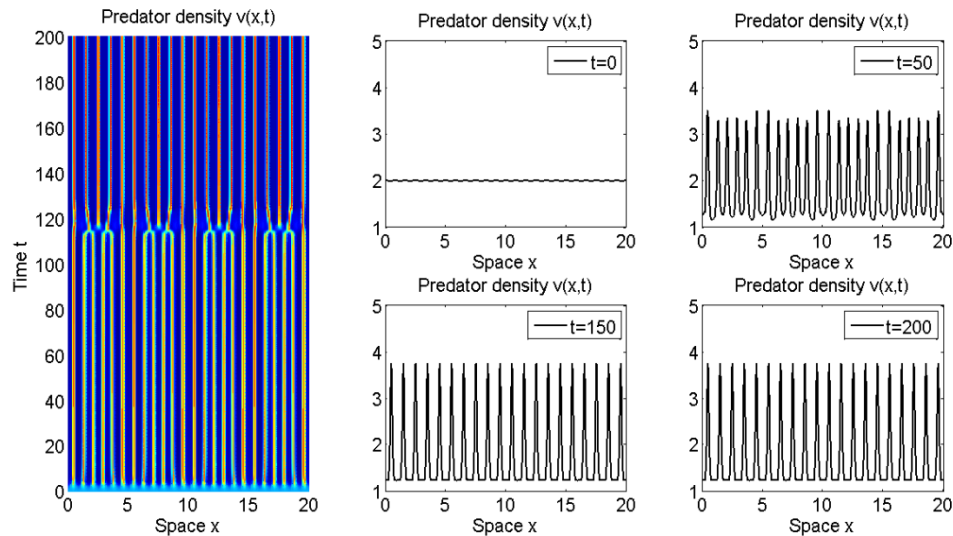


FIGURE 6. Merging and emerging phenomena during the formation of stationary pattern in (5) over $\Omega = (0, 20)$. System parameters are chosen $d_1 = 0.1$, $d_2 = 0.1$, $a = 10$, $b = 2$, $c = 0.1$, $d = 27$, $e = 30$, $h = 1.5$ and $\chi = 0.185$, $M = 0.1$. We observe that merging and emerging phenomena occurs at time $t \approx 120$ s.

authors thank three referees for their kind and helpful comments which improve the presentation of this paper.

References

- [1] B.E. Aïnseba, M. Bendahmane and A. Noussair, A reaction–diffusion system modeling predator–prey with prey–taxis, *Nonlinear Anal. Real World Appl.*, 9 (2008), 2086–2105.
- [2] K.-S. Cheng, Uniqueness of a limit cycle for a predator–prey system, *SIAM J. Math. Anal.*, 12 (1981), 541–581.
- [3] A. Chertock, A. Kurganov, X. Wang and Y. Wu, On a chemotaxis model with saturated chemotactic flux, *Kinet. Relat. Models*, 5 (2012), 51–95.
- [4] C. Cosner, Reaction–diffusion–advection models for the effects and evolution of dispersal, *Discrete Contin. Dyn. Syst.*, 34 (2014), 1701–1745
- [5] M.G. Crandall and P.H. Rabinowitz, Bifurcation from simple eigenvalues, *J. Functional Analysis*, 8 (1971), 321–340.
- [6] M.G. Crandall and P.H. Rabinowitz, Bifurcation, perturbation of simple eigenvalues, and linearized stability, *Arch. Rational Mech. Anal.*, 52 (1973), 161–180.
- [7] S.R. Dunbar, Traveling waves in diffusive predator–prey equations: periodic orbits and point-to-periodic heteroclinic orbits, *SIAM J. Appl. Math.*, 46 (1986), 1057–1078.
- [8] S.I. Ei, H. Izuhara and M. Mimura, Spatio–temporal oscillations in the Keller–Segel system with logistic growth, *Phys. D*, 277 (2014), 1–21.
- [9] H.I. Freedman, *Deterministic Mathematical Models in Population Ecology*, Marcel Dekker, New York, 1980.
- [10] M. R. Garvie and C. Trenchea, Spatiotemporal dynamics of two generic predator–prey models, *J. Biol. Dyn.*, 4 (2010), 559–570.
- [11] G. Gerisch, Chemotaxis in dictyostelium, *Ann. Rev. Phys.*, 44 (1982), 535–552.
- [12] Z. M. Gliwicz, P. Maszczyk, J. Jablonski and D. Wrzosek, Patch exploitation by planktivorous fish and the concept of aggregation as an antipredation defense in zooplankton, *Limnology and Oceanography*, 58 (2013), 1621–1639.
- [13] P. Haastert and P. Devreotes, Chemotaxis: signalling the way forward, *Nature Reviews Molecular Cell Biology*, 5 (2004), 626–634.

- [14] X. He and S. Zheng, Global boundedness of solutions in a reaction–diffusion system of predator–prey model with prey–taxis, *Appl. Math. Lett.*, 49 (2015), 73–77.
- [15] T. Hillen and K. J. Painter, A user’s guidance to PDE models for chemotaxis, *J. Math. Biol.*, 58 (2009), 183–217.
- [16] S.-B. Hsu and J. Shi, Relaxation oscillator profile of limit cycle in predator–prey system, *Discrete Contin. Dyn. Syst. Ser. B*, 11 (2009), 893–911.
- [17] S.-B. Hsu, S.P. Hubbell and P. Waltman, Competing predators, *SIAM J. Appl. Math.*, 35 (1978), 617–625.
- [18] J. Jang, W.-M. Ni and M. Tang, Global bifurcation and structure of Turing patterns in the 1-D Lengyel–Epstein model, *J. Dynam. Differential Equations*, 16 (2004), 297–320.
- [19] P. Kareiva and G. Odell, Swarms of predators exhibit “preytaxis” if individual predators use area–restricted search, *The American Naturalist*, 130, (1987), 233–270.
- [20] T. Kato, *Functional Analysis*, Springer Classics in Mathematics, 1996.
- [21] E.F. Keller and L.A. Segel, Initiation of slime mold aggregation viewed as an instability, *J. Theoret. Biol.*, 26 (1970), 399–415.
- [22] E.F. Keller and L.A. Segel, Model for Chemotaxis, *J. Theoret. Biol.*, 30 (1971), 225–234.
- [23] E.F. Keller and L.A. Segel, Traveling bands of chemotactic bacteria: A Theoretical Analysis, *J. Theoret. Biol.*, 30 (1971), 235–248.
- [24] K. Kishimoto and H. Weinberger, The spatial homogeneity of stable equilibria of some reaction–diffusion systems in convex domains, *J. Differential Equations*, 58 (1985), 15–21.
- [25] K. Kuto, Stability of steady–state solutions to a prey–predator system with cross–diffusion, *J. Differential Equations*, 197 (2004), 293–314.
- [26] K. Kuto and Y. Yamada, Multiple coexistence states for a prey–predator system with cross–diffusion, *J. Differential Equations*, 197 (2004), 315–348.
- [27] K.-Y. Lam and D. Munther, Invading the ideal free distribution, *Discrete Contin. Dyn. Syst. Ser. B*, 19 (2014), 3219–3244.
- [28] K.-Y. Lam and Y. Lou, Evolution of conditional dispersal: evolutionarily stable strategies in spatial models, *J. Math. Biol.*, 68 (2014), 851–877.
- [29] J.M. Lee, T. Hillen and M.A. Lewis, Continuous traveling waves for prey–taxis, *Bull. Math. Biol.*, 70 (2008), 654–676.
- [30] J.M. Lee, T. Hillen and M.A. Lewis, Pattern formation in prey–taxis systems, *J. Biol. Dyn.*, 3 (2009), 551–573.
- [31] C. Li, X. Wang and Y. Shao, Steady states of a predator–prey model with prey–taxis, *Nonlinear Anal.*, 97 (2014), 155–168.
- [32] M. Ma, C. Ou and Z.-A. Wang, Stationary solutions of a volume filling chemotaxis model with logistic growth and their stability, *SIAM J. Appl. Math.*, 72 (2012), 740–766.
- [33] M. Ma and Z.-A. Wang, Global bifurcation and stability of steady states for a reaction–diffusion–chemotaxis model with volume–filling effect, *Nonlinearity*, 28 (2015), 2639–2660.
- [34] R.M. May, Limit cycles in predator–prey communities, *Science*, 177 (1972) 900–902.
- [35] R.M. May, “Stability and Complexity in Model Ecosystems”, Princeton Univ. Press, 1974
- [36] A.B. Medvinsky, S.V. Petrovskii, I.A. Tikhonova, H. Malchow and B.-L. Li, Spatiotemporal complexity of plankton and fish dynamics, *SIAM Rev.*, 44 (2002), 311–370.
- [37] K. Nakashima and Y. Yamada, Positive steady states for prey–predator models with cross–diffusion, *Adv. Differential Equations*, 1 (1996), 1099–1122.
- [38] K. Painter and T. Hillen, Volume-filling and quorum-sensing in models for chemosensitive movement, *Can. Appl. Math. Q.*, 10 (2002), 501–543.
- [39] K. Painter and T. Hillen, Spatio–temporal chaos in a chemotaxis model, *Phys. D*, 240 (2011), 363–375.
- [40] C. S. Patlak, Random walk with persistence and external bias, *Bull. Math. Biophys.*, 15 (1953), 311–338.
- [41] P. H. Rabinowitz, Some global results for nonlinear eigenvalue problems, *J. Funct. Anal.*, 7 (1971), 487–513.
- [42] S. Rinaldi, S. Muratori and Y. Kuznetsov, Multiple attractors, catastrophes and chaos in seasonally perturbed predator–prey communities, *Bull. Math. Bio.*, 55 (1993), 15–35.
- [43] M.L. Rosenzweig and R. MacArthur, Graphical representation and stability conditions of predator–prey interactions, *Amer. Natur.*, 97 (1963), 209–223.
- [44] K. Ryu and I. Ahn, Positive steady–states for two interacting species models with linear self–cross diffusions, *Discrete Contin. Dyn. Syst.*, 9 (2003), 1049–1061.
- [45] D. H. Sattinger, Bifurcation and symmetry breaking in applied mathematics, *Bull. Amer. Math. Soc.*, 3 (1980), 779–819.

- [46] J. Shi and X. Wang, On global bifurcation for quasilinear elliptic systems on bounded domains, *J. Differential Equations*, 246 (2009), 2788–2812.
- [47] G. Simonett, Center manifolds for quasilinear reaction–diffusion systems, *Differential Integral Equations*, 8 (1995), 753–796.
- [48] Y. Tao, Global existence of classical solutions to a predator–prey model with nonlinear prey–taxis, *Nonlinear Anal. Real World Appl.*, 11 (2010), 2056–2064.
- [49] K. Wang, Q. Wang and F. Yu, Stationary and time periodic patterns of two-predator and one-prey systems with prey–taxis, *Discrete Contin. Dyn. Syst.*, 37 (2017), 505–543.
- [50] Q. Wang, On the steady state of a shadow system to the SKT competition model, *Discrete Contin. Dyn. Syst. Ser. B*, 19 (2014), 2941–2961.
- [51] Q. Wang, C. Gai and J. Yan, Qualitative analysis of a Lotka–Volterra competition system with advection, *Discrete Contin. Dyn. Syst.*, 35 (2015), 1239–1284.
- [52] Q. Wang, Y. Song and L. Shao, Nonconstant positive steady states and pattern formation of 1D prey–taxis systems, *J. Nonlinear Sci.*, 27 (2017), 71–97.
- [53] Q. Wang, J. Yang and L. Zhang, Time periodic and stable patterns of a two-competing-species Keller–Segel chemotaxis model: effect of cellular growth, *Discrete Contin. Dyn. Syst. Ser. B*, 22 (2017), 3547–3574.
- [54] Q. Wang, L. Zhang, J. Yang and J. Hu, Global existence and steady states of a two competing species Keller–Segel chemotaxis model, *Kinet. Relat. Models*, 8 (2015), 777–807.
- [55] X. Wang, W. Wang and G. Zhang, Global bifurcation of solutions for a predator–prey model with prey–taxis, *Math. Methods Appl. Sci.*, 38 (2015), 431–443.
- [56] X. Wang and Q. Xu, Spiky and transition layer steady states of chemotaxis systems via global bifurcation and Helly’s compactness theorem, *J. Math. Biol.*, 66 (2013), 1241–1266.
- [57] F. Yi, J. Wei and J. Shi, Bifurcation and spatiotemporal patterns in a homogeneous diffusive predator–prey system, *J. Differential Equations*, 246 (2009) 1944–1977.
- [58] M. Yousefnezhad and A. Mohammadi, Stability of a predator–prey system with prey taxis in a general class of functional responses, *Acta Math. Sci.*, 36 (2016), 62–72.

School of Securities and Futures, Southwestern University of Finance and Economics, 555 Liutai Ave, Wenjiang, Chengdu, Sichuan 611130, China
E-mail: yyzhang@swufe.edu.cn

Department of Mathematics, Guangdong University of Finance and Economics, Guangzhou 510320, China.
E-mail: xaleysherry@163.com